

Research Article

Optimal Inspection Scheduling Model for Monitoring Railway Track Grids

Qing Li ¹, Ling Liu ^{1,2}, Rengkui Liu ³, and Lei Bai ⁴

¹Beijing National Railway Research & Design Institute of Signal & Communication Group Co., Ltd., Beijing 100070, China

²Beijing Engineering Technology Research Center of Operation Control Systems for High Speed Railways, Beijing 100070, China

³School of Traffic and Transportation, Beijing Jiaotong University, Beijing 100044, China

⁴Jiuzhouyigui Environmental Technology Co., Ltd., Beijing 100070, China

Correspondence should be addressed to Lei Bai; bailei@bjtu.edu.cn

Received 31 December 2021; Accepted 21 April 2022; Published 25 May 2022

Academic Editor: Wen-Tsao Pan

Copyright © 2022 Qing Li et al. This is an open access article distributed under the Creative Commons Attribution License, which permits unrestricted use, distribution, and reproduction in any medium, provided the original work is properly cited.

The optimization of railway track inspection schedules is of great significance for the monitoring of railway track conditions and reasonable organization of track maintenance tasks. Here, an optimal inspection scheduling model for monitoring railway tracks is proposed. Railway track inspection activities are divided into equal-length units in the time and spatial location dimensions. The various constraints and objectives on the time and location of different track inspection activities are defined in detail regarding subdivisions of individual management units. The objectives of the model development are to achieve a more optimized equilibrium and robustness of the track inspection schedule. Based on the maximum entropy criterion, entropy is used to measure the distribution equilibrium of the inspection schedule in the time dimension. The proposed model is verified using actual data from the Lanxin railway.

1. Introduction

Following the development of high-speed railways, the safety and continuous operation of trains and comfortable travel of passengers necessitate the reliability, stability, and durability of railway track systems. A railway track is a structure composed of multiple components and is classified into two types: ballasted and ballastless tracks [1]. The ballasted track consists of rails, sleepers, fasteners, and ballast. Slab ballastless tracks and double-block ballastless tracks are mainly used in China's high-speed railways. The slab ballastless track consists of rails, fasteners, slab tracks, cement-emulsified asphalt mortar, and baseplates [2]. The railway track system is a long and large linear asset that is categorized as civil infrastructure and not electrical equipment. Therefore, the achievement of real-time online monitoring of the condition of the entire track system is difficult and costly.

Track inspection comprises both on-track and on-board inspections for track geometry and track component inspection [3]. According to the rules of railway track

maintenance [4–6], inspection activities of various inspection methods for railway track systems should be scheduled and organized scientifically and rationally. Ensuring that managers are aware of the condition of railway tracks in time and effectively organize maintenance operations is critical. Common track inspection methods include track geometry cars, track geometry trolleys, cabin-mounted track quality instruments, portable track quality instruments, rail detection trolleys, and manual track walking inspection. On-track inspections include track geometry trolleys and manual track walking inspections among others, whereas on-board inspections include track geometry cars and portable track quality instruments, among others.

Optimizing the equilibrium of the time intervals between adjacent inspection activities and overall robustness are the main challenges experienced in the scheduling of track inspection activities. The equilibrium of the time intervals between adjacent inspection activities indicates that the time intervals of different inspection activities should be as balanced as possible. In addition T_j , T_{j+1} , T_{j+2} , T_{j+3} , and T_{j+4}

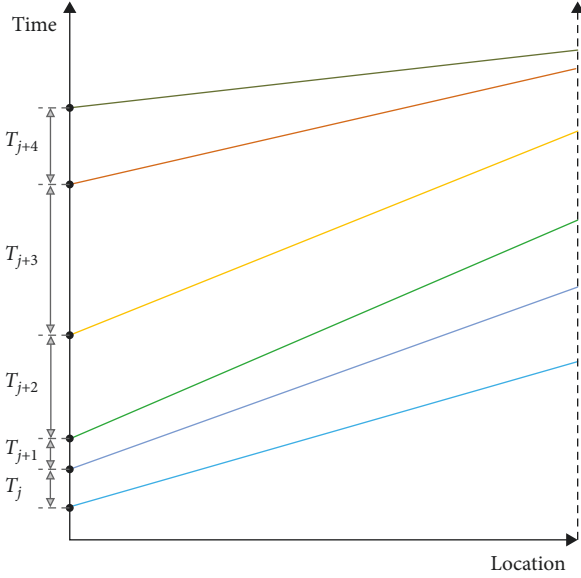


FIGURE 1: Diagram of adjacent inspection intervals for different inspection activities.

should be as equal as possible, as shown in Figure 1. Improved equilibrium allows for a more optimized distribution of inspections, thereby preventing inspections that are spaced out within too long a period or that are too frequent within a short period. The robustness of the inspection schedule refers to the ability to reduce the effects of various random disturbances (such as severe weather conditions) on the schedule during the execution process. Moreover, $\min(T_j, T_{j+1}, T_{j+2}, T_{j+3}, T_{j+4})$ should be as large as possible. Improved robustness can increase the flexibility of the inspection schedule in the start or end time variation of inspection activities and prevent delays and advances in inspection activities that disrupt the organization of resources such as labor, materials, and machines, as shown in Figure 1. In Figure 1, the horizontal axis represents the location along the railway track, the vertical axis represents the date of inspection activities, and the solid lines with different colors represent different inspection activities.

Currently, research on the optimization of transportation infrastructure inspection schedules mainly focuses on the following two aspects. (1) In a certain scheduling period, the optimal inspection frequency for the transportation infrastructure using the same inspection method and the inspection interval between two adjacent inspection activities are studied [7–17]. These studies assume that the inspection workload and inspection frequency of the transportation infrastructure are not fixed periodically.

Liu [7] aimed to minimize the risk of derailment in the transportation of dangerous goods and proposed a rail inspection frequency optimization model to determine the optimal annual inspection frequency for different railway segments under different risk levels. Soleimanmeigouni et al. [8] proposed a cost-based track geometry inspection interval optimization model to determine the time interval between adjacent inspections of the track geometry in a scheduling cycle. Liu et al. [9] proposed an optimization model for a rail

detection trolley inspection schedule with the optimal objectives of optimizing traffic safety, cost, and transportation efficiency. This model determines the number of rail detection inspections in a scheduling period and the detection time interval for two adjacent rail detection inspections with a known number of detection times.

Khouy et al. [10] proposed an optimization model for track geometry inspection intervals, with the minimum cost (including inspection cost, fault repair cost, preventive maintenance cost, and potential risk cost) corresponding to the unit gross tonnage as the optimization objective. Podofillini et al. [11] proposed an optimization model of rail detection schedule using risk-informed approaches and reliability-based approaches and determined the inspection interval of two adjacent rail detection inspections with the optimization objectives of cost and safety. Using the structural reliability theory, Kashima [12] proposed an optimization model for the inspection interval of rail detection inspection based on the life cycle cost. Vatn and Svee [13] proposed a risk-based optimization model for rail detection inspection intervals, and their optimization objective was to minimize cost.

Lam and Banjevic [14] proposed a decision policy for condition-based maintenance that schedules inspections according to the current health of the system, optimized myopically over the subsequent inspection interval. Yan et al. [15] proposed and optimized a nonfixed periodic inspection strategy with a warning degradation threshold, whose optimization objectives were the application of the warning threshold and inspection interval. In the proposed strategy, the above warning threshold is categorized as a degradation process divided into two parts: normal and warning areas, where two different inspection intervals can be used. When the equipment is in normal areas, the corresponding inspection interval is long. When the equipment is in the warning areas, the corresponding inspection interval is short. Kim and Frangopol [16] proposed a cost-based inspection and monitoring optimization model for fatigue-sensitive structures using a probabilistic approach. The inspection schedule is the solution to an optimization problem to minimize the expected total cost (including inspection cost and expected failure cost) and determine the number of inspections and the interval between two adjacent inspections within a planning cycle. Yang and Xie [17] proposed a discrete-time SMDP-based decision-making approach for determining optimal MR&R strategy and inspection intervals for infrastructure facilities, resulting in cost savings and reducing unnecessary waste of resources.

Using the model predictive control (MPC) approach, Su et al. [18] developed a scenario-based chance-constrained approach for railway condition-based maintenance planning, minimizing disruption cost and setup cost of maintenance slots for a finite planning horizon. Further advancing this research, Su et al. [19] proposed a multilevel decision-making approach for both optimal long-term condition-based maintenance planning and optimal short-term maintenance crew scheduling, minimizing condition deterioration and maintenance costs. The MPC and mixed-integer linear programming (MILP) approaches were used.

(2) The optimal selection of different inspection methods for transportation infrastructure at different decision-making stages in a certain planning horizon has been studied [20–22]. These studies assume that the transportation infrastructure manager adopts a fixed periodic inspection strategy. Only one inspection activity was selected from a finite set for each decision-making stage. The finite set consists of different inspection activities wherein different instruments are used. Multiple inspection activities cannot be selected during the same decision-making stage.

Madanat and Ben-Akiva [20] adopted the latent Markov decision process to determine the types of inspection and maintenance activities at different decision-making moments of road surfaces in a long planning cycle, considering the difference in inspection errors and inspection costs of different inspection methods. Durango-Cohen and Samer M [21], considering the uncertainty of road surface state degradation, dynamically adjusted the weight system of the finite known Markov state degradation model using the quasi-Bayes approach to describe the regulation of road surface state degradation. The latent Markov decision process method is used to determine the types of inspection and maintenance activities at different decision moments in a long planning cycle. Mishalani and Gong [22] established the functional relationship between the inspection error of different inspection methods of road surfaces and the uncertainty of their spatial sampling and determined the inspection activity type and maintenance activity type of road surfaces at different decision-making times in a long planning cycle using the hidden Markov decision process method.

In this study, railway track inspection activities were divided into same-length units in the time and spatial location dimensions to consider the influence of various heterogeneous factors (such as geological conditions and climatic conditions). Based on the features of railway track inspection activities, and to optimize the equilibrium and robustness of rail track systems, a time-location grid-based optimal inspection scheduling model for monitoring railway tracks is proposed. The constraint system includes time constraint between activities, fixed duration constraint, spatial constraint between activities, rate constraint of activities, resource constraint, and continuity constraint.

Three fundamental perspectives distinguish our study from previous investigations. (1) This study proposes a method for the definition and division of time-location grids. We divide railway track inspection activities into same-length units in the time and spatial location dimensions. Various constraints and objectives on the time and spatial location of different track inspection activities are defined in great detail with regard to subdivisions of individual management units. (2) A time-location grid-based optimal inspection scheduling model is proposed, with the optimization objectives of attaining equilibrium and robustness. This model enhances the practicability of the inspection schedule, reduces the influence of various factors on the inspection schedule, and guarantees the management of the actual inspection activities on-site. (3) Based on the maximum entropy criterion, entropy is used to measure the

distribution equilibrium of adjacent inspection activity intervals in the inspection schedule.

The remainder of this paper is organized as follows. In Section 2, we analyze the features of railway track inspection activities, explain the concept of time-location grids for railway tracks, and present the time-location grid-based optimal inspection scheduling model for monitoring railway tracks. A validation of the proposed model, conducted using actual measurement data, is presented in Section 3. Our conclusions are presented in Section 4.

2. Features of Railway Track Inspection Activities

Although there are many types of railway track inspection methods with varying inspection principles, railway track inspection activities generally have the following characteristics.

- (1) Railway track inspection activities are continuous in the horizontal direction. Generally extending from one end of the line segment to the other, track inspection activities are mainly composed of activities with repetitive features. For example, the inspection activity of a track geometry trolley is generally carried out continuously and repeatedly in multiple line segments, which consumes time and advances continuously in accordance with the mileage position.
- (2) The inspection items of the different inspection methods are consistent. For example, the inspection items of track geometry cars and track geometry trolleys include surface, alignment, gauge, cross-level, and twist. The rail detection car, rail detection trolley, and manual inspection all inspect rail defects.
- (3) To ensure the safety of the operator, the inspection activities of certain inspection methods should be scheduled within the maintenance window, such as the inspection of the track geometry trolley and rail detection trolley. At the same time, certain inspection activities such as the inspection of track geometry cars and rail detection cars do not need to be scheduled within the maintenance window.
- (4) There is no logical constraint on the sequence of inspection activities with different inspection methods in the time dimension; that is, the sequence of inspection activities with different inspection methods does not affect the perception of track condition.
- (5) There are no multiple inspection activities within a temporal-spatial location. For example, when carrying out inspection activities involving rail detection trolleys, it is not possible to arrange inspection activities involving track geometry trolleys at the same location.
- (6) The inspection activities are affected by various temporal-spatial factors, such as the line segment with high risk and hidden danger of equipment

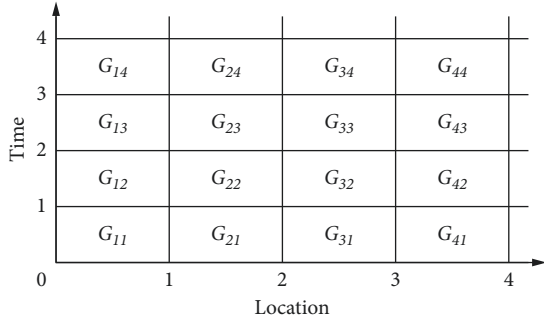


FIGURE 2: Diagram of railway time-location grid.

quality, and the frequency of inspection activities should be increased. The inspection speed is uncertain owing to a variety of temporal-spatial factors.

3. Subdivision of Railway Track Inspection Activity Based on Time-Location Grid

Railway grid [23] refers to dividing the linear, continuous, and strip-shaped railway lines dividing railway track inspection activities into equal-length “small segments” according to certain rules. The railway time-location grid [24] refers to several small units formed by dividing the entire life cycle process of railway infrastructure based on time and spatial dimensions according to certain rules, as shown in Figure 2. The horizontal axis represents the location and the vertical axis represents time. Each time-location grid is represented by G_{ij} , where i represents the i^{th} railway grid, and j represents the time period when the grid is located. The railway time-location grid is a temporal-spatial-based basic unit and is divided as follows:

- (1) Time grid division: According to the actual work requirements of railway infrastructure management, the life cycle process of railway infrastructure can be divided based on minutes, hours, days, weeks, months, and years in the time dimension. In different application scenarios, the administrator can choose the size of the time grid unit based on the actual scenario requirements.
- (2) Location grid division: As the smallest unit for dividing linear and continuous railway lines in the spatial dimension, the division of the location grid should take full account of the operation characteristics of inspection activities and the management needs of the railway site, the length of the railway grid in the study is set at 200 m, and the 100 m railway sign is selected as the demarcation point for adjacent grids.

Railway track inspection activities have a clear time span and mileage range information and consume a certain amount of time and resources. Based on the railway time-location grid, the railway track inspection activities are divided into smaller time and spatial units, which can more precisely define various constraints on the time and location of inspection activities, and more accurately illustrate the

influence of various time and spatial factors on inspection activities. Therefore, railway infrastructure inspection activities with relatively high temporal and spatial resolutions are manageable, as shown in Figure 3. The horizontal axis represents the location and the vertical axis represents time. The blue line represents the inspection activities of railway infrastructure. The angle between the blue line and the horizontal axis indicates the rate of activity execution. The smaller the angle, the faster the execution rate of the corresponding activities. The red shaded part in Figure 3(b) represents the temporal-spatial constraints between any time and mileage point in the entire execution process of two adjacent activities.

4. Time-Location Grid-Based Optimal Inspection Scheduling Model for Monitoring Railway Track

4.1. Constant. The constants involved in the time-location grid-based optimal inspection scheduling model for monitoring railway track (TGOISM-MRT) are outlined as follows (Table 1):

4.2. Decision Variables. The decision variable of the TGOISM-MRT is t_{ij}^e , which indicates whether the track grid G_i performs the inspection activity of the inspection method C_j in the e^{th} unit time, $t_{ij}^e \in [0, 1]$, as shown in equation (1). $t_{ij}^e = 1$ indicates that the track grid G_i performs the inspection activity of the inspection method C_j in the e^{th} unit time. As $t_{ij}^e = 0$, the track grid G_i does not perform the inspection activity of the inspection method C_j in the e^{th} unit time.

$$t_{ij}^e = \begin{cases} 1, & \text{Inspection activity is performed} \\ 0, & \text{Inspection activity is not performed.} \end{cases} \quad (1)$$

For inspection method C_j , the corresponding optimization problem has $N \times E$ Boolean decision variables to be considered, as shown in Figure 4. There are M types of inspection methods for the entire model; therefore, the TGOISM-MRT has a total of $M \times N \times E$ Boolean decision variables that need to be considered.

4.3. Decision Expression. The decision expression involved in the TGOISM-MRT is as follows.

Z_{ij} represents a set of execution times of the previous inspection activities of inspection method C_j of track grid G_i in a scheduling cycle. The number of elements in set Z_{ij} is equal to the inspection time threshold S_{ij} of the C_j is the j^{th} inspection method and G_i the i^{th} track grid. The elements in set Z_{ij} are represented by z_{ij}^n , $n \in [1, 2, \dots, S_{ij}]$, and z_{ij}^n indicating that track grid G_i performs the inspection activity of method C_j in the z_{ij}^n -th unit time. The functional relationship between z_{ij}^n and t_{ij}^e ($e \in [1, 2, \dots, E]$) is illustrated by equation (2). $t_{ij}^e \neq 0$ indicates that track grid G_i performs the inspection activity of the inspection method C_j in the e^{th} unit time, and $z_{ij}^n = e$.

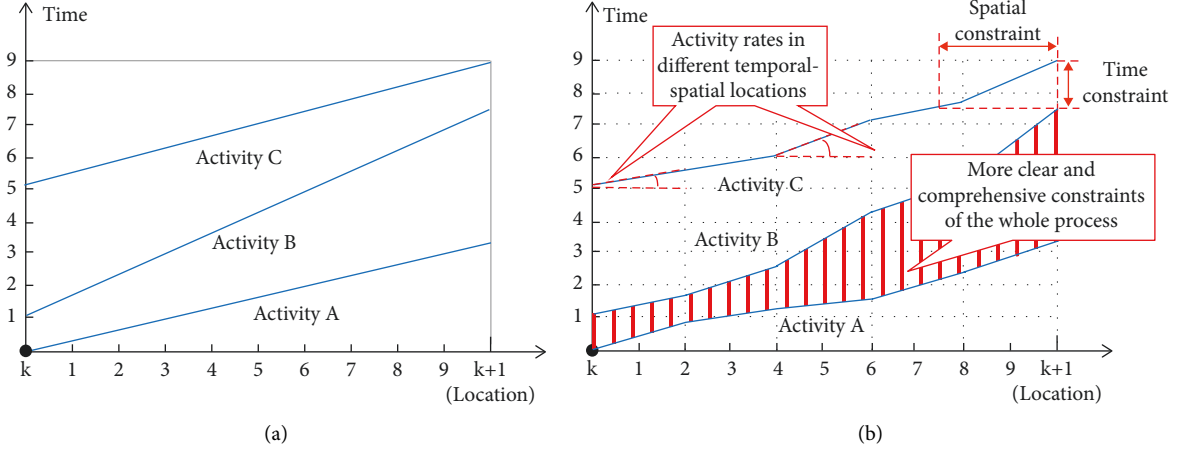


FIGURE 3: Comparison of the condition before and after subdivision of railway track inspection activities based on the time-location grid. (a) Diagram of railway inspection schedule. (b) Diagram of time-location grid-based railway inspection schedule.

TABLE 1: Variable denotations.

SD	Starting mileage of the inspection schedule
ED	Ending mileage of the inspection schedule
DR	$= ED - SD$, which represents the mileage length of the inspection activity
LE	Length of the track grid is generally 200 m
N	$= DR/LE$ represents the total number of track grids divided by railway lines
$G_i (i \in [1, 2, \dots, N])$	i^{th} track grid
M	Total number of types of track inspection methods
$C_j (j \in [1, 2, \dots, M])$	j^{th} inspection method
$C_{ij} (i \in [1, 2, \dots, N], j \in [1, 2, \dots, M])$	j^{th} inspection method of track grid G_i
E	Total unit time in a scheduling cycle
S_{ij}	Inspection time threshold of the j^{th} inspection method C_j of the i^{th} track grid G_i in a scheduling cycle
S_i	Owing to the influence of various temporal and spatial factors, the inspection frequency values of the same inspection method may differ for different track grids $= \sum_{j=1}^M S_{ij}$ which represents the inspection time threshold of the total number of inspection methods of track grid G_i in a scheduling cycle
$\min T_{ij}$	Minimum inspection interval threshold of inspection method C_j of track grid G_i in the scheduling cycle
$\max T_{ij}$	Maximum inspection interval threshold C_j of track grid G_i inspection method in a scheduling cycle
$\max L_j$	Threshold of the maximum number of grids inspected in the inspection method C_j per unit time
$\min L_j$	Threshold of the minimum number of grids inspected in the inspection method C_j per unit time
RC_j	Number of workgroups performing inspection activities with an inspection method C_j
RC	Total number of workgroups performing inspection activities

$$z_{ij}^n = \text{Inf} \{e | t_{ij}^e \neq 0, e \in [1, 2, \dots, E]\}. \quad (2)$$

U_i represents a set of execution times of the previous inspection activities of all inspection methods of track grid G_i in a scheduling cycle. The number of elements in set U_i is equal to the inspection time threshold S_i of the total number of inspection methods of track grid G_i . The elements in set U_i are represented by u_i^m , $m \in [1, 2, \dots, S_i]$, and u_i^m indicating that the track grid G_i performs the inspection activity of method C_j in the u_i^m -th unit time. The functional relationship between u_i^m and t_{ij}^e ($e \in [1, 2, \dots, E]$) is expressed in equation (3). $t_{ij}^e \neq 0$ indicates that track grid G_i performs the inspection activity of inspection method C_j in the e^{th} unit time, and $u_i^m = e$.

$$u_i^m = \text{Inf} \{e | t_{ij}^e \neq 0, e \in [1, 2, \dots, E], j \in [1, 2, \dots, M]\}. \quad (3)$$

Q_{ij} represents the inspection times of inspection method C_j of track grid G_i and is calculated as follows.

$$Q_{ij} = \sum_{e=1}^E t_{ij}^e. \quad (4)$$

v_j^e represents the number of grids inspected by inspection method C_j in the e^{th} unit time and is calculated as follows.

$$v_j^e = \sum_{i=1}^N t_{ij}^e. \quad (5)$$

	Time 1	Time 2	Time e	Time E
1	0	1	0	1
2	1	0	0	0
.
.
.
i	t_{ij}^e	1	.
.
.
.
N	0	0	1	0	0	0

FIGURE 4: Schematic of decision variable t_{ij}^e .

R_j^e represents the number of workgroups required to perform inspection activities using inspection method C_j in the e^{th} unit time and is calculated as follows. The TGOISM-MRT assumes that there is only one workgroup for the inspection activity using method C_j . If there are multiple workgroups for inspection method C_j , the actual problem is divided into several subproblems of a single workgroup according to the inspection task.

$$R_j^e = \text{Inf} \left(1 \left| \sum_{i=1}^N t_{ij}^e > 0 \right. \right). \quad (6)$$

4.4. Objective Functions Based on Time-Location Grid

4.4.1. Equilibrium Objective Function. The TGOISM-MRT uses entropy theory to construct an index called time entropy that measures the equilibrium of the track inspection schedule in the time dimension. The greater the time entropy, the more balanced the inspection schedule in the time dimension.

“Information Entropy” or “Shannon Entropy” [25] was first proposed by Claude Elwood Shannon in 1948 to measure the uncertainty of information. When the state or result of the event is known, information entropy H is equal to 0, where the greater the possibility of states or results of an event, the greater the uncertainty, and the greater the H . The mathematical abstraction of information entropy H is that an event has n possible results X_i ($i \in [1, 2, \dots, n]$), and the probability of each result is p_i . Information entropy H , which measures the uncertainty of the event, is calculated as follows.

$$H = - \sum_{i=1}^n p_i \ln p_i, \quad (7)$$

$$\sum_{i=1}^n p_i = 1, \quad i \in [1, 2, \dots, n],$$

$$p_i \geq 0, \quad i \in [1, 2, \dots, n].$$

Based on the maximum entropy criterion [26], when p_i ($i = 1, 2, 3, \dots, n$) satisfies the following conditions, H in equation (7) is at its maximum value. Therefore, entropy is a remarkable index for measuring the degree of a group of data, partial to the system mean. The smaller the entropy, the greater the deviation of the set of data from the mean. The greater the entropy, the more concentrated the data is around the mean, and the more balanced the distribution of the data. When a set of data is completely equal, the entropy value reaches its maximum value.

$$p_1 = p_2 = \dots = p_n = \frac{1}{n}. \quad (8)$$

The TGOISM-MRT replaces variable p_i in equation (8) and redefines entropy as p_i^n determined as the ratio of the time interval b_i^n between two adjacent inspection activities and the total number of unit times $E - 1$ in the scheduling cycle. This entropy is called the time entropy, TH_i , of track grid G_i and is used as the equilibrium index to measure the time interval between two adjacent inspection activities of track grid G_i in a scheduling cycle, as shown in equation (11). The larger the value of the time entropy TH_i , the more balanced the time interval between two adjacent inspection activities in the inspection schedule. b_i^n represents the time interval between the $n + 1^{\text{th}}$ inspection activity and the n^{th} inspection activity of the track grid G_i , as shown in equation (12). p_i^n represents the ratio of b_i^n to the total number of unit times $E - 1$ in the scheduling cycle, as shown in equation (13), where $i \in [1, 2, \dots, N]$, and $n \in [1, 2, \dots, S_i - 1]$. $E - 1$ is used to define p_i^n because the sum of all $S_i - 1$ time intervals b_i^n in the scheduling cycle of track grid G_i is equal to $E - 1$.

$$TH_i = - \sum_{n=1}^{S_i-1} p_i^n \ln p_i^n, \quad (9)$$

$$b_i^n = u_i^{n+1} - u_i^n,$$

$$p_i^n = \frac{b_i^n}{E - 1}.$$

According to the maximum entropy criterion, when the time entropy TH_i of track grid G_i reaches the maximum value, p_i^n ($n \in [1, 2, \dots, S_i - 1]$) values are equal to each other. That is, in a scheduling cycle, the larger the value of time entropy TH_i , the closer the time interval value of two adjacent inspection activities in track grid G_i , and the higher the equilibrium degree of the scheduled inspection of track grid G_i .

The time entropy of all track grids of the railway line is expressed by TH , which is used to measure the equilibrium of all track grids of railway lines in a scheduling cycle, and is calculated as follows.

$$TH = \sum_{i=1}^N TH_i = - \sum_{i=1}^N \sum_{n=1}^{S_i-1} p_i^n \ln p_i^n. \quad (10)$$

When the time entropy TH of the entire railway line reaches the maximum value, the time entropy TH_i of track

grid $G_i (i \in [1, 2, \dots, N])$ reaches the maximum value, and the inspection schedule equilibrium degree of each track grid in the entire railway line is at its highest.

According to the maximum entropy criterion, the ideal maximum value $TH_{i,\max}$ of time entropy TH_i of track grid G_i without considering the task constraints is expressed as follows.

$$TH_{i,\max} = - \sum_{n=1}^{S_i-1} \frac{(E-1/S_i-1)}{E-1} \ln \left(\frac{(E-1/S_i-1)}{E-1} \right) = - \ln \left(\frac{1}{S_i-1} \right). \quad (11)$$

Accordingly, the ideal maximum value, TH_{\max} , of TH of all track grids of the railway line is shown in

$$TH_{\max} = \sum_{i=1}^N TH_{i,\max} = - \sum_{i=1}^N \ln \frac{1}{S_i-1}. \quad (12)$$

The ratio of the time entropy TH of all the track grids of the railway line to its ideal maximum value TH_{\max} is expressed by the THR, as shown in

$$THR = \frac{TH}{TH_{\max}}. \quad (13)$$

The equilibrium objective function of TGOISM-MRT is shown in

$$\max THR. \quad (14)$$

4.4.2. Robust Objective Function. The robustness of the inspection schedule refers to the ability to reduce the effects of various random disturbances during the execution process. Owing to the influence of time and spatial factors (such as severe weather and holidays), railway track inspection activities may be delayed or canceled temporarily, which may easily lead to chaos in the entire track inspection schedule. Therefore, the prepared inspection schedule can reduce the influence of various random disturbances.

The TGOISM-MRT defines robust, R , as the ratio of the minimum time interval between two adjacent inspection activities in the track grid to the total unit time E in a scheduling cycle. It is considered to be an important index for measuring the flexibility of the inspection schedule and is calculated as follows.

$$R = \min \frac{b_i^n}{E}, \forall i \in [1, 2, \dots, N], \forall n \in [1, 2, \dots, S_i - 1]. \quad (15)$$

The robust objective function of TGOISM-MRT is shown in

$$\max R. \quad (16)$$

4.4.3. Weight-Based Multiobjective Function. The TGOISM-MRT can achieve multiobjective optimization of the equilibrium and robustness of the time interval between adjacent inspection activities of the inspection schedule. Using weighted summation, the multiobjective optimization

problem is transformed into a single-objective optimization problem. The optimal objective function after the transformation of TGOISM-MRT is shown in equation (17), where α and β are the weights of the two objective functions. The values of α and β are set by the manager according to the importance of the objectives of equilibrium and are robust in the actual situation.

$$\max \alpha THR + \beta R, \quad (17)$$

where

$$\begin{aligned} \alpha + \beta &= 1, \\ 0 \leq \alpha, \beta &\leq 1. \end{aligned} \quad (18)$$

4.5. Constraint System Based on Time-Location Grid. This subsection defines the following six types of inspection activity constraints based on the time-location grid of railway track: time constraints between activities, fixed duration constraints, spatial constraints between activities, rate constraints of activities, resource constraints, and continuity constraints, as shown in Figure 5.

4.5.1. Time Constraint between Activities. As shown in Figure 5(a), the time constraints between track inspection activities are as follows. ① In a scheduling cycle, the time interval of inspection method C_j of track grid G_i should be greater than or equal to the minimum inspection interval threshold $\min T_{ij}$, as shown in equation (21). ② In a scheduling cycle, the time interval of inspection method C_j of track grid G_i should be less than or equal to the maximum inspection interval threshold $\max T_{ij}$, as shown in equation (22). In an inspection scheduling cycle, if the inspection time specified by a certain inspection method is 1, the time constraint of the inspection activity corresponding to the inspection method is not considered. In Figure 5(a), the horizontal axis represents the railway mileage, the vertical axis represents the time, and the solid lines of different colors represent different inspection activities. The horizontal axis is divided by the length of the grid, and the vertical axis is divided by the time granularity required for management to form the track time-location grid.

$$\begin{aligned} z_{ij}^{m+1} - z_{ij}^m &\geq \min T_{ij} \forall m \in [1, 2, \dots, S_{ij} - 1], \\ z_{ij}^{m+1} - z_{ij}^m &\leq \max T_{ij} \forall m \in [1, 2, \dots, S_{ij} - 1]. \end{aligned} \quad (19)$$

The violation of the maximum time constraint hinders the identification of quality-related problems in the track by managers, and violation of the minimum time constraint results in a waste of inspection resources.

4.5.2. Fixed Duration Constraint. The fixed duration constraint for track inspection activities includes two aspects. ① In a scheduling cycle, each type of inspection method needs to complete the specified number of inspections. ② The inspection activities of each type of inspection method involve inspecting all track grids to avoid missing inspections.

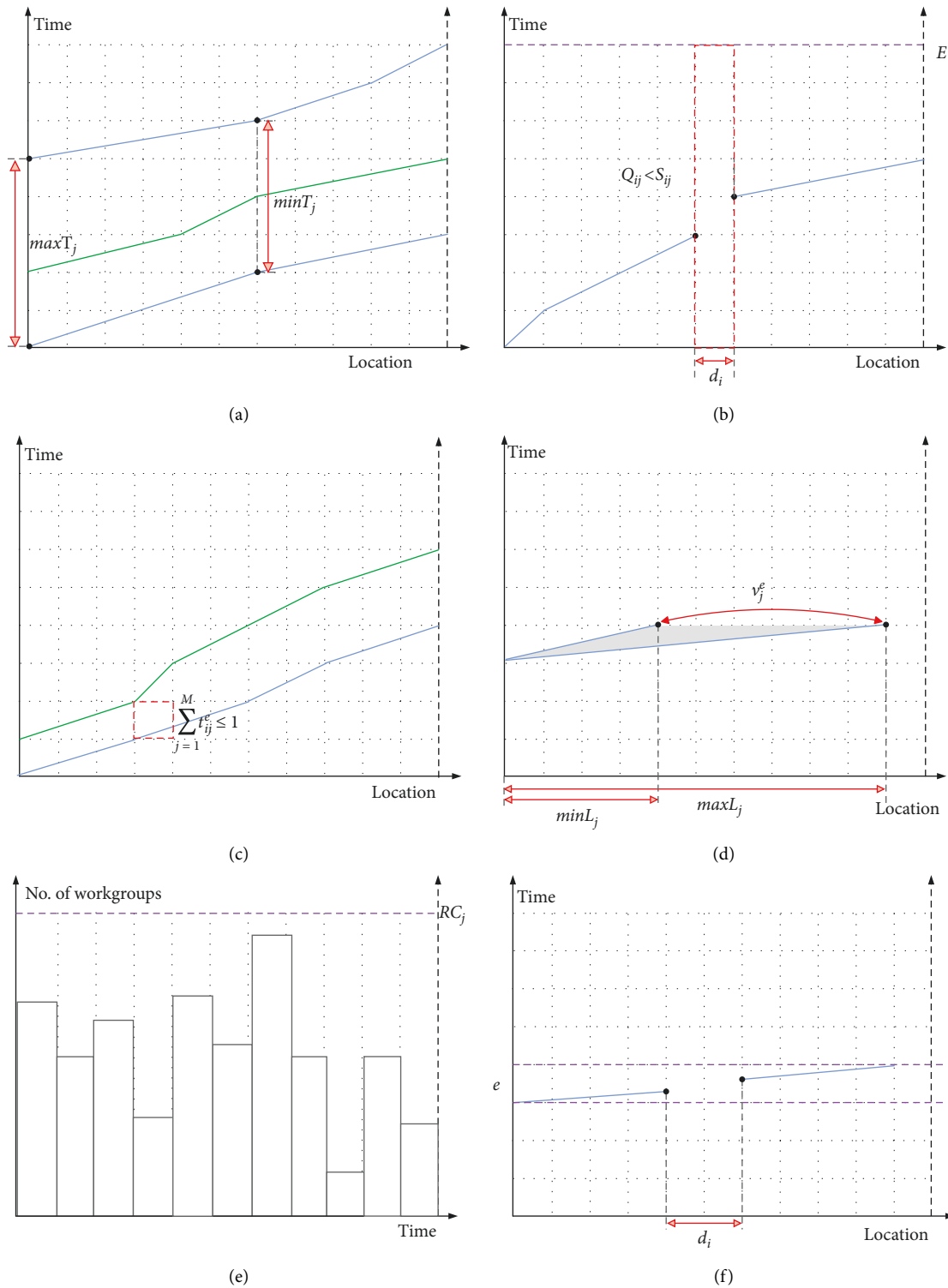


FIGURE 5: Map of time-location grids based on various constraints of track inspection activities. (a) Time constraint between activities. (b) Fixed duration constraint. (c) Spatial constraint between activities. (d) Rate constraint of activities. (e) Resource constraint. (f) Continuity constraint.

Therefore, in a scheduling cycle, the number of inspection times Q_{ij} of the inspection method C_j of the track grid G_i should be equal to the inspection time threshold S_{ij} . In Figure 5(b), the horizontal axis represents the railway

mileage, and the vertical axis represents the time. The horizontal axis is divided by the length of the grid, and the vertical axis is divided by the time granularity required for management to form the track time-location grid. The

purple dotted line indicates the deadline of the inspection schedule. In the figure, owing to the existence of $d_i > 0$, the dotted frame area $Q_{ij} < S_{ij}$, which does not meet the fixed duration constraint.

$$Q_{ij} = S_{ij} \forall i \in [1, 2, \dots, N], j \in [1, 2, \dots, M]. \quad (20)$$

The violation of the fixed duration constraint causes the track line without risk to evolve into potential risk, and the original low risk may evolve into a high risk.

4.5.3. Spatial Constraint between Activities. The spatial constraint of track inspection activities means that at most one inspection activity can occur in any time-location grid of the railway track. That is, at most, one inspection activity can occur in track grid G_i per unit time, as shown in equation (21) and Figure 5(c). In Figure 5(c), the horizontal axis represents the railway mileage, the vertical axis represents the time, and the solid lines of different colors represent different inspection activities. The horizontal axis is divided by the length of the grid, and the vertical axis is divided by the time granularity required for management to form the track time-location grid.

$$\sum_{j=1}^M t_{ij}^e \leq 1 \forall i \in [1, 2, \dots, N], e \in [1, 2, \dots, E]. \quad (21)$$

If the above constraints are violated, time-location conflicts between inspection activities occur, affecting the efficiency and safety of inspection activities.

4.5.4. Rate Constraint of Activities. The TGOISM-MRT defines the inspection rate by the number of grids inspected in inspection method C_j per unit time of each type of inspection activity. As shown in Figure 5(d), the rate constraint between track inspection activities is as follows. ①The number of grids inspected v_j^e in inspection method C_j per unit time should be less than or equal to the maximum rate threshold $\max L_j$, as shown in equation (22). ②The number of grids inspected v_j^e in inspection method C_j per unit time should be greater than or equal to the maximum rate threshold $\min L_j$, as shown in equation (23). In Figure 5(d), the horizontal axis represents the railway mileage, and the vertical axis represents the time. The horizontal axis is divided by the length of the grid, and the vertical axis is divided by the time granularity required for management to form the track time-location grid.

$$v_j^e \leq \max L_j \forall e \in [1, 2, \dots, E], j \in [1, 2, \dots, M], \quad (22)$$

$$v_j^e \geq \min L_j \forall e \in [1, 2, \dots, E], j \in [1, 2, \dots, M]. \quad (23)$$

The maximum rate constraint is used to guarantee inspection quality and prevent false and missed inspections. The minimum rate constraint is used to ensure the efficiency of inspection activities.

4.5.5. Resource Constraint. The resource constraint of track inspection activities means that the number of inspection

activities R_j^e with inspection method C_j in unit time is less than or equal to the corresponding number of workgroups RC_j , as shown in equation (24) and Figure 5(e). In Figure 5(e), the horizontal axis represents the railway mileage, and the vertical axis represents the time. The horizontal axis represents the number of workgroups. The purple dotted line indicates the RC_j resource usage threshold.

$$R_j^e \leq RC_j \forall e \in [1, 2, \dots, E]. \quad (24)$$

Meeting the resource constraints is the basic guarantee of the feasibility of the inspection schedule. If the amount of resources used by the inspection activities exceeds that of the available resources, the organization and arrangement of inspection activities will be unsuccessful.

4.5.6. Continuity Constraint. The continuity constraint of railway track inspection means that the inspection activities performed by each working group with inspection method C_j must be continuous and uninterrupted within a unit time, as shown in equation (25) and Figure 5(f). In Figure 5(f), the horizontal axis represents the railway mileage, and the vertical axis represents the time. The horizontal axis is divided by the length of the grid, and the vertical axis is divided by the time granularity required for management to form the track time-location grid. The purple dotted line indicates the start and end times of the e^{th} unit time. Owing to the existence of $d_i > 0$ in the figure, the continuity constraint is not satisfied.

$$\sum_{i=p}^{p+v_j^e-1} t_{ij}^e = v_j^e \forall e \in [1, 2, \dots, E], \exists p \in [1, 2, \dots, N]. \quad (25)$$

If the above constraints are violated, the inspection activities will be discontinuous or interrupted, which will result in a waste of resources, loss of inspection efficiency, and increased management costs.

5. Results and Discussion

5.1. Overview of Empirical Analysis. Actual data regarding the track inspection schedule were collected from December 2016 on a segment in the downward direction of the Lanxin railway between 721 and 765 km. The proposed model was verified using accumulated data.

DR represents the segment length between 721 and 765 km in the downward direction of the Lanxin railway and spans 44 km. This railway segment passed through the Jiayuguan and Heishanhu stations. The center mileage of the Jiayuguan station is 737.954 km. The center mileage of Heishanhu station was 759.319 km. The Jiayuguan Department is a subsidiary branch under the jurisdiction of the China Railway Lanzhou Group that offers inspection and maintenance services. LE represents the length of the track grid: LE = 200 m. Therefore, the total number of track grids, N , considered in this study is $DR/LE = 220$.

In this study, an inspection schedule was prepared on a monthly basis. E represents the total number of days in a

TABLE 2: Workload of track inspection activities for December 2016 in the Lanxin railway.

No.	C_j	j	Direction	SD (km)	ED (km)	Sets of track grid	DR (km)	S_{ij}	$\max T_{ij}$ (day)	$\min T_{ij}$ (day)
1	Track geometry trolley inspection	1	Down	721	765	[1, 2, ..., 220]	44	1	35	15
2	Rail detection trolley inspection	2	Down	721	765	[1, 2, ..., 220]	44	1	35	15
3	Manual inspection	3	Down	721	730	[1, 2, ..., 45]	9	1	35	15
4	Manual inspection	3	Down	730	736	[46, 47, ..., 75]	6	2	18	7
5	Manual inspection	3	Down	736	765	[76, 77, ..., 220]	24	1	35	15
6	Track geometry car inspection	4	Down	721	765	[1, 2, ..., 220]	44	2	18	7

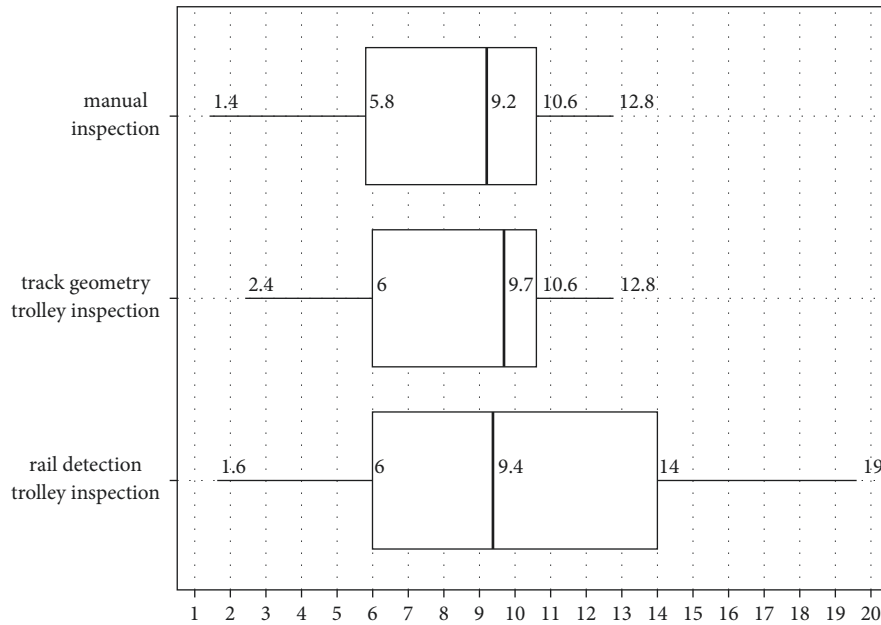


FIGURE 6: Box plot of activity rates of different inspection methods.

scheduled cycle and is calculated to be 31. Four track inspection methods were considered, including a track geometry trolley, rail detection trolley, manual inspection, and track geometry car. The workload of track inspection activities for the Jiayuguan Department in the downward direction of the Lanxin railway in December 2016 is shown in Table 2. The track quality of the segment between 731 and 736 km in the downward direction of the Lanxin railway is poor. Therefore, the manual inspection frequency of the track grids within the mileage ranging between 731 and 736 km is one more time than the manual inspection frequency of other track grids. The track geometry car inspection was prearranged on December 8th and 21st, respectively, for the first and second inspections in the downward direction of the Lanxin railway.

The Jiayuguan Department has four groups: Workgroup 1 is responsible for track geometry trolley inspections; Workgroup 2 is responsible for rail detection trolley inspections; Workgroup 3 is responsible for manual inspection; Workgroup 4 is responsible for track geometry car inspections.

To obtain the inspection rate for the inspection methods, 581 historical inspection rate data for the four workgroups between January 2015 and December 2017 (three years) were

collected. These data were analyzed using box plot methods to observe the overall distribution of these data and identify possible outliers. The first and third quartiles in the historical inspection rate data were selected as the upper and lower thresholds of the inspection rate for the inspection methods.

The inspection rate was defined as the railway line length inspected per unit of maintenance time. The box plot of the activity rates for different inspection methods is shown in Figure 6, where the horizontal axis indicates the inspection activity rate, and the vertical axis indicates the type of inspection method. The rate constraints of the different inspection methods are listed in Table 3.

5.2. Analysis of Results. The First Optimization (1stOpt) software [27] was used to solve the combined optimization problem of the TGOISM-MRT. Parameter α in the objective function was 0.5 and parameter β was 0.5. After the calculation, the corresponding optimal objective function value was 0.570. The equilibrium THR for the track inspection schedule was 0.980. The robust R of track inspection was 0.161. The execution time is approximately two hours, and the statistic was collected using a desktop with an Intel E5-1620 3.50-GHz CPU and 16 GB RAM.

TABLE 3: Rate constraints of different inspection methods.

No.	Workgroups	C_j	j	$\min L_j$		$\max L_j$	
				km per maintenance window	Number of track grids per maintenance window	km per maintenance window	Number of track grids per maintenance window
1	Workgroup 1	Track geometry trolley inspection	1	6	30	10.6	53
2	Workgroup 2	rail detection trolley inspection	2	6	30	14	70
3	Workgroup 3	Manual inspection	3	5.8	29	10.6	53
4	Workgroup 4	Track geometry car inspection	4	The track geometry car GJ-5 lacks a power source and needs to be hung at the end of the passenger train, to detect track irregularities. Its inspection rate depends on the speed of the passenger train.			

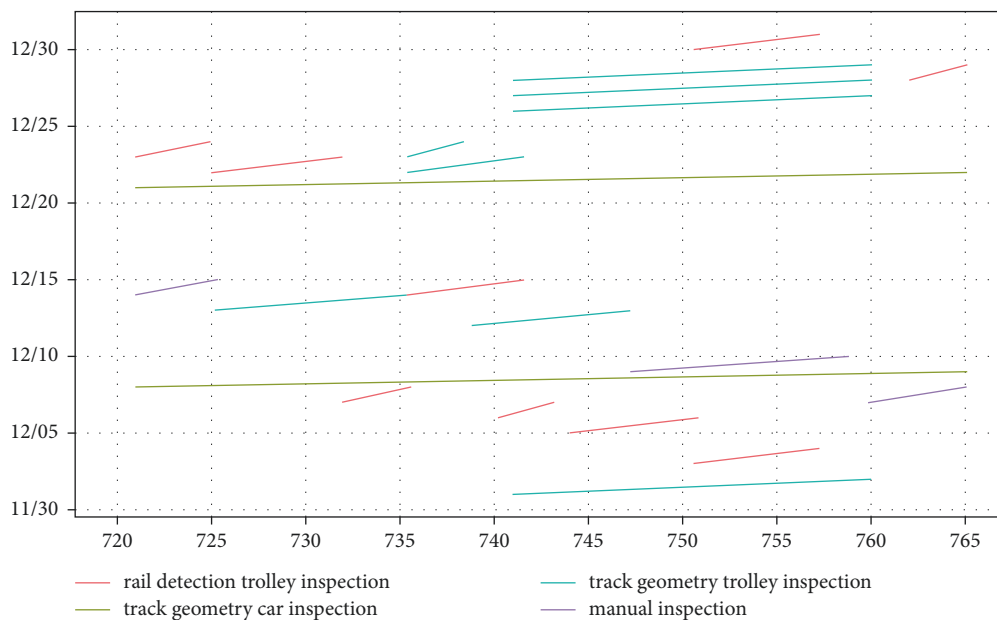


FIGURE 7: Actual track inspection schedule in the Lanxin railway.

The actual track inspection schedule for the Lanxin railway in December 2016 is shown in Figure 7. The track inspection schedule for December 2016 in the Lanxin railway using the OISM-RTG model is shown in Figure 8. In Figures 7 and 8, the horizontal axis represents the railway mileage, the vertical axis represents the time, and the solid lines of different colors represent different inspection activities. The solid red line indicates the inspection activities of the rail detection trolley. The solid green line indicates the inspection activity of the track geometry car. The solid blue line indicates the inspection activity of the track geometry trolley. The solid purple line indicates manual inspection activities.

A comparison of the pre- and postoptimized track inspection schedules is shown in Table 4. Table 4 shows the following:

- (1) Constraints: The actual track inspection schedule in the empirical analysis does not satisfy the fixed

duration constraint, space constraint between activities, and rate constraint of activities. This is because the track inspection schedule is mainly based on the management experience of field engineers. It is difficult for these engineers to comprehensively and systematically consider the track inspection activity constraint system established in this study.

- (2) Objective function: Compared with the actual track inspection schedule, the track inspection schedule using the TGOISM-MRT improves the equilibrium THR by 22.5%. The robust R increases from 0 to 0.161. The corresponding weighted objective function value was enhanced by 42.5%.

In summary, combined with the visual presentation results of Figures 7 and 8, the track inspection schedule using the TGOISM-MRT is superior to the actual inspection schedule prepared by the field engineer, with a more optimized equilibrium THR and robust R .

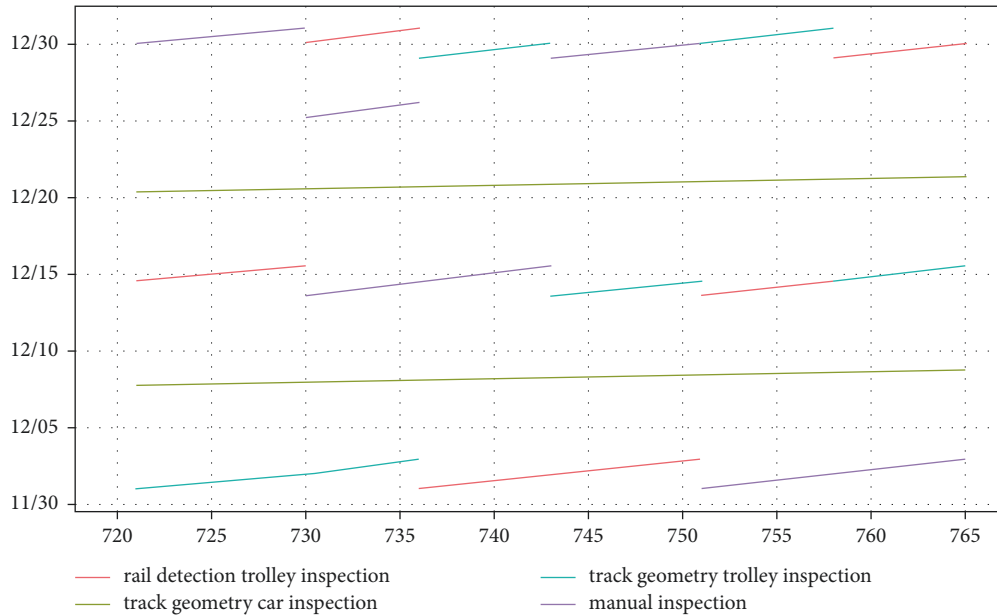


FIGURE 8: Track inspection schedule in the Lanxin railway using model TGOISM-MRT.

TABLE 4: Comparison of actual and optimized track inspection schedule.

Item	Inspection schedule using the OISM-RTG	Actual inspection schedule prepared by the field engineers
Constraint system	Time constraints between activities	Satisfaction
	Fixed duration constraint	Satisfaction
	Space constraints between activities	Violation. For example, the rail detection trolley inspection is not scheduled for track segments between 757.2 and 762 km in the downward direction of the Lanxin railway.
	Rate constraint of activities	Violation. For example, on December 26th, the track geometry trolley inspection is scheduled for track segments between 741 and 760 km in the downward direction of the Lanxin railway. The inspection rate is 19 km per maintenance window and is nearly double the upper inspection rate limit (10.6 km per maintenance window).
	Resource constraint	Satisfaction
Objectives	Continuity constraint	Satisfaction
	Equilibrium THR	0.980
	Robust r	0.161
	Weighted objective function	0.570
Visual presentation results	A comparison of Figures 7 and 8 shows that the inspection schedule using the TGOISM-MRT model is superior to the actual inspection schedule prepared by the field engineers.	

6. Conclusions

This study analyzed the features of railway track inspection activities and proposed TGOISM-MRT for optimal inspection scheduling of railway tracks. Track time-location grids were the subject of this study. Time-location grid-based objectives and constraint systems for different track inspection activities are constructed. The TGOISM-MRT is optimized for the equilibrium and robustness of the track inspection schedule to ensure the practicality and guidance

of the track inspection schedule. Constraint systems include time constraints between activities, fixed duration constraints, space constraints between activities, rate constraints of activities, resource constraints, and continuity constraints.

The proposed model was verified using actual data for segments ranging between 721 and 765 km in the downward direction of the Lanxin railway. Compared with the actual inspection schedule prepared by the field engineers, the track inspection schedule using the TGOISM-MRT can satisfy the

proposed constraint system and yields more optimized equilibrium and robustness.

The TGOISM-MRT proposed in this paper can also be employed to solve the optimization of the inspection schedule of other linear assets (such as highways and pipelines), with little modification. To improve the TGOISM-MRT and promote the flexibility and practicability of the track inspection schedule, further research will be carried out.

- (1) Owing to the assumption limitations of the TGOISM-MRT, the model is suitable for the optimization of the inspection schedule for a single line. Optimizing the track inspection schedule for large-scale railway networks can be a future research direction.
- (2) The implementation of the railway track inspection schedule will continue for a period of time. The progress control of the inspection schedule is a process of continuous circular adjustment of the schedule. The optimization of the progress control of the inspection schedule will be explored in future research studies.

Data Availability

Previously reported data are used to support this study and are cited at relevant places within the text as references.

Conflicts of Interest

The authors declare no conflicts of interest regarding the publication of this paper.

Acknowledgments

This work was supported by the National Natural Science Foundation of China (grant no. U1834209) and the National Key R&D Program of China (grant no. 2017YFB1200700). The authors are grateful for the kind support and cooperation of the China Railway Lanzhou Bureau Group Co., Ltd. in providing valuable data. The authors would like to thank Editage (<http://www.editage.cn>) for English language editing.

References

- [1] E. B. O. C. Encyclopedia, *Encyclopedia of China Railway*, China Railway Publishing House, Beijing, China, 1st edition, 2004.
- [2] G. Liang, *Track Engineering*, China Railway Publishing House, Beijing, China, 2nd edition, 2015.
- [3] L. Bai, R. Liu, and Q. Li, "Data-driven bias correction and defect diagnosis model for in-service vehicle acceleration measurements," *Sensors*, vol. 20, no. 3, p. 872, 2020.
- [4] The Railway Ministry of China, *Railway Transport [2006] No. 146 Rules of Railway Track Maintenance*, Railway Publishing House, Beijing, China, 2010.
- [5] The Railway Ministry of China, *Railway Transport. [2012] No. 83 Interim Rules of High-Speed Railway Ballastless Track Maintenance*, Railway Publishing House, Beijing, China, 2012.
- [6] The Railway Ministry of China, *Railway Transport. [2013] No. 29 Interim Rules of High-Speed Railway Ballast Track Maintenance*, Railway Publishing House, Beijing, China, 2013.
- [7] X. Liu, "Optimizing rail defect inspection frequency to reduce the risk of hazardous materials transportation by rail," *Journal of Loss Prevention in the Process Industries*, vol. 48, pp. 151–161, 2017.
- [8] I. Soleimanmeigouni, A. Ahmadi, C. Letot, A. Nissen, and U. Kumar, "Cost-based optimization of track geometry inspection," in *Proceedings of the 11th World Congress of Railway Research*, Milan, Italy, June 2016.
- [9] X. Liu, A. Lovett, T. Dick, M. Rapik Saat, and C. P. L. Barkan, "Optimization of ultrasonic rail-defect inspection for improving railway transportation safety and efficiency," *Journal of Transportation Engineering*, vol. 140, no. 10, Article ID 4014048, 2014.
- [10] I. A. Khouy, P.-O. Larsson-Kräik, A. Nissen, U. Juntti, and H. Schunnesson, "Optimisation of track geometry inspection interval," *Proceedings of the Institution of Mechanical Engineers - Part F: Journal of Rail and Rapid Transit*, vol. 228, no. 5, pp. 546–556, 2014.
- [11] L. Podofillini, E. Zio, and J. Vatn, "Risk-informed optimisation of railway tracks inspection and maintenance procedures," *Reliability Engineering & System Safety*, vol. 91, no. 1, pp. 20–35, 2006.
- [12] T. Kashima, *Reliability-based Optimization of Rail Inspection*, Massachusetts Institute of Technology, Cambridge, 2004.
- [13] J. Vatn and H. A. Svee, "Risk based approach to determine ultrasonic inspection frequencies in railway applications," in *Proceedings of the 22nd ESReDA Seminar*, Madrid, Spain, May 2002.
- [14] J. Y. J. Lam and D. Banjevic, "A myopic policy for optimal inspection scheduling for condition based maintenance," *Reliability Engineering & System Safety*, vol. 144, pp. 1–11, 2015.
- [15] H.-C. Yan, J.-H. Zhou, and C. K. Pang, "Cost optimization on warning threshold and non-fixed periodic inspection intervals for machine degradation monitoring," in *Proceedings of the IECON 2015 - 41st Annual Conference of the IEEE Industrial Electronics Society*, Yokohama, Japan, November 2015.
- [16] S. Kim and D. M. Frangopol, "Cost-based optimum scheduling of inspection and monitoring for fatigue-sensitive structures under uncertainty," *Journal of Structural Engineering*, vol. 137, no. 11, pp. 1319–1331, 2011.
- [17] Y. Yang and H. Xie, "Determination of optimal MR&R strategy and inspection intervals to support infrastructure maintenance decision making," *Sustainability*, vol. 13, no. 5, pp. 1–10, 2021.
- [18] Z. Su, A. Jamshidi, A. Núñez, S. Baldi, and B. De Schutter, "Multi-level condition-based maintenance planning for railway infrastructures - a scenario-based chance-constrained approach," *Transportation Research Part C: Emerging Technologies*, vol. 84, pp. 92–123, 2017.
- [19] Z. Su, A. Jamshidi, A. Núñez, S. Baldi, and B. De Schutter, "Integrated condition-based track maintenance planning and crew scheduling of railway networks," *Transportation Research Part C: Emerging Technologies*, vol. 105, pp. 359–384, 2019.
- [20] S. Madanat and M. Ben-Akiva, "Optimal inspection and repair policies for infrastructure facilities," *Transportation Science*, vol. 28, no. 1, pp. 55–62, 1994.
- [21] P. L. Durango-Cohen and S. M. Madanat, "Optimization of inspection and maintenance decisions for infrastructure facilities under performance model uncertainty: a quasi-Bayes

- approach,” *Transportation Research Part A: Policy and Practice*, vol. 42, no. 8, pp. 1074–1085, 2008.
- [22] R. G. Mishalani and L. Gong, “Optimal infrastructure condition sampling over space and time for maintenance decision-making under uncertainty,” *Transportation Research Part B: Methodological*, vol. 43, no. 3, pp. 311–324, 2009.
- [23] R. Liu, L. Bai, F. Wand, Q. Sun, and F. Wang, “Grid: a new theory for high-speed railway infrastructure management,” in *Proceedings of the Transportation Research Board 94th Annual Meeting*, Washington DC, United States, January 2015.
- [24] Q. Li, *Time-location Grid-Based Optimal Inspection Scheduling and Repair Planning Model for Railway Track*, Beijing Jiaotong University, Beijing, China, 2018.
- [25] C. E. Shannon, “A mathematical theory of communication,” *Bell System Technical Journal*, vol. 27, no. 3, pp. 379–423, 1948.
- [26] E. T. Jaynes, “Information theory and statistical mechanics,” *Physical Review*, vol. 106, no. 4, pp. 620–630, 1957.
- [27] X. Cheng, F. Chai, J. Gao, and K. Zhang, “1st opt and global optimization platform-comparison and case study,” in *Proceedings of the 4th IEEE International Conference on Computer Science and Information Technology*, Chengdu, China, March 2011.